Letter

Interplay of thermal and nonthermal effects in x-ray-induced ultrafast melting

Ichiro Inoue,[1,2,*] Victor Tkachenko,[3,4,†] Yuya Kubota,[1] Fabien Dorchies,[5] Toru Hara,[1] Hauke Höppner,[6] Yuichi Inubushi,[1,7] Konrad J. Kapcia,[4,8] Hae Ja Lee,[9] Vladimir Lipp,[4,10] Paloma Martinez,[5] Eiji Nishibori,[11,12] Taito Osaka,[1] Sven Toleikis,[13] Jumpei Yamada,[1] Makina Yabashi,[1,7] Beata Ziaja,[4,10,‡] and Philip A. Heimann[9,§]

[1]*RIKEN SPring-8 Center, 1-1-1 Kouto, Sayo, Hyogo 679-5148, Japan*
[2]*University of Hamburg, Institute for Experimental Physics/CFEL, Luruper Chaussee 149, 22761 Hamburg, Germany*
[3]*European XFEL GmbH, Holzkoppel 4, 22869 Schenefeld, Germany*
[4]*Center for Free-Electron Laser Science CFEL, Deutsches Elektronen-Synchrotron DESY, Notkestr. 85, 22607 Hamburg, Germany*
[5]*Université de Bordeaux, CNRS, CEA, Centre Lasers Intenses et Applications, UMR 5107, 33400 Talence, France*
[6]*Helmholtz-Zentrum Dresden-Rossendorf, 01328 Dresden, Germany*
[7]*Japan Synchrotron Radiation Research Institute, Kouto 1-1-1, Sayo, Hyogo 679-5198, Japan*
[8]*Institute of Spintronics and Quantum Information, Faculty of Physics and Astronomy, Adam Mickiewicz University in Poznań, Uniwersytetu Poznańskiego 2, 61614 Poznań, Poland*
[9]*SLAC National Accelerator Laboratory, Menlo Park, California 94025, USA*
[10]*Institute of Nuclear Physics, Polish Academy of Sciences, Radzikowskiego 152, 31-342 Krakow, Poland*
[11]*Graduate School of Pure and Applied Sciences, University of Tsukuba, Tsukuba, Ibaraki 305-8571, Japan*
[12]*Faculty of Pure and Applied Sciences and Tsukuba Research Center for Energy Materials Science, University of Tsukuba, Tsukuba, Ibaraki 305-8571, Japan*
[13]*Deutsches Elektronen-Synchrotron DESY, Notkestr. 85, 22607 Hamburg, Germany*

(Received 28 August 2023; revised 6 August 2024; accepted 13 August 2024; published 27 September 2024)

X-ray laser-induced structural changes in silicon undergoing femtosecond melting have been investigated by using an x-ray pump–x-ray probe technique. The experiment reveals that the atomic displacements start to increase at ∼20 fs after the intensity maximum of x-ray pump pulse. By comparing the observed time dependence of the atomic disordering and the dedicated theoretical simulations, we interpret that the energy transfer from the excited electrons to ions via electron-ion coupling (thermal effect) as well as a strong modification of the interatomic potential due to electron excitations (nonthermal effect) trigger the ultrafast atomic disordering. Our results highlight the need to consider the interplay of thermal and nonthermal effects in the quantitative modeling of the interaction of intense x rays with matter.

DOI: 10.1103/PhysRevB.110.L100102

Ultrafast laser pulses can bring matter into highly nonequilibrium states and induce exotic processes. The well-known example is femtosecond melting, which is often called nonthermal melting. It has been observed in various semiconductors [1–12] and in two-dimensional materials [13,14] irradiated with femtosecond optical laser pulses, where the excitation of a large fraction (more than a few percent) of the valence electrons modifies the interatomic potential and drives ultrafast atomic disordering without equilibrium between the electron and ion subsystems [15].

The recent advent of x-ray free-electron lasers (XFELs) [16,17], emitting intense femtosecond x-ray pulses, has extended these studies to the x-ray regime. Understanding the physics governing the x-ray-induced ultrafast melting is of great importance in the context of practical applications of XFELs, particularly the structure determination of nanocrystals [18,19]. While x-ray nanocrystallography of organic molecules and proteins is challenging with conventional light sources due to radiation damage during x-ray exposure [20–23], the short duration of the XFEL pulses allows measurement of the diffraction signal before the manifestation of radiation damage [24]. In those experiments, the XFEL pulses are focused down to a micrometer size or even less so that the beam size matches the crystal size. Since irradiation with focused XFEL pulses inevitably excites many valence electrons [25–27], setting the pulse duration to be shorter than the onset time of the atomic disordering is essential for the success of such experiments.

The mechanism of x-ray-induced atomic disordering still remains unclear. For example, the x-ray-induced femtosecond melting in silicon (Si) has been intensively studied both experimentally [28,29] and theoretically [27,30], but the detailed mechanism of the disordering processes is still under debate. An x-ray pump–x-ray probe experiment [28] demonstrated that the root-mean-square (rms) atomic displacements in Si, when excited slightly above the damage threshold, increase with time at a constant rate nearly equal to the velocity of atoms in the equilibrium state ($\sqrt{3k_BT/m}$, where k_B is the

*Contact author: inoue@spring8.or.jp
†Contact author: victor.tkachenko@xfel.eu
‡Contact author: beata.ziaja-motyka@cfel.de
§Contact author: paheim@slac.stanford.edu

 ©2024 American Physical Society

Boltzmann constant, T is the sample temperature before x-ray excitation, and m is the mass of the atom). The authors of Ref. [28] claimed that electron excitations triggered by x-ray exposure flatten the interatomic potential surface and drive inertial atomic motion, a phenomenon similar to femtosecond melting in semiconductors under weak excitation [7]. In another experiment, Hartley *et al.* [29] measured the time-resolved diffuse scattering of Si after irradiation with an intense XFEL pulse (corresponding to an x-ray dose more than ten times higher than the damage threshold). By comparing the experimental results with simulations, they concluded that the modified interatomic potential due to electron excitation ("nonthermal effect") is the key factor dominating the speed of atomic disordering. Recent numerical simulations that investigated the damage threshold of x-ray-induced ultrafast melting in various materials [30–32] suggested that not only the nonthermal effect but also the energy transfer from the excited electrons to ions via electron-ion coupling ("thermal effect") may contribute to the atomic disordering on the femtosecond timescale.

In experiments involving structure determination with XFEL pulses, the x-ray dose absorbed by the sample is far above the damage threshold [18,19,24]. Unveiling the onset time and mechanism of atomic disordering for materials exposed to intense x-ray pulses under high radiation dose conditions is crucial for the accurate interpretation of experimental results. In order to elucidate the impact of the three aforementioned factors (thermal effect, nonthermal effect, and initial equilibrium atomic motion) on the atomic disordering, we measured XFEL-induced structural changes in Si under strong excitation conditions at various temperatures by using an x-ray pump–x-ray probe technique [26,33,34]. By exploiting XFEL pulses from SACLA with a duration of much below 10 fs [35–39], we captured the initial stage of the atomic disordering.

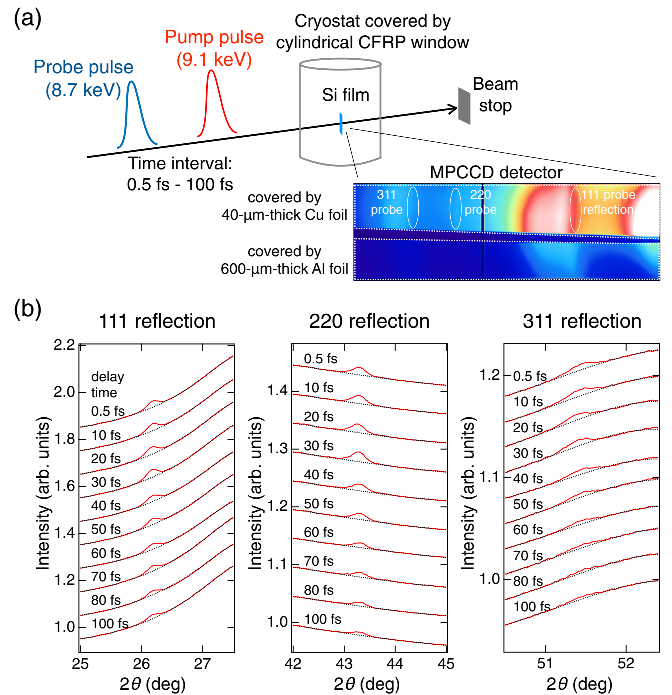

FIG. 1. (a) A schematic illustration of the experiment. (b) The diffraction profiles of probe pulses for silicon at 300 K. For better visibility, each diffraction profile is linearly shifted along the vertical axis. The black dotted lines show the estimated background.

Figure 1(a) shows a schematic illustration of the experimental setup at SACLA BL3 [40]. The XFEL machine was operated to generate 9.10-keV pump and 8.70-keV probe pulses with an rms duration of 2.5 fs by a split-undulator scheme [41]. Since the jitter of the time interval between the double pulse was much less than 1 fs [41], the x-ray pulse duration determined the time resolution of the measurement ($\sqrt{2} \times 2.5$ fs $= 3.6$ fs). The pump and probe pulses were focused to full width at half maximum (FWHM) sizes of 1.8 μm (horizontal) × 1.8 μm (vertical) and 1.0 μm (horizontal) × 1.4 μm (vertical), respectively, by using an x-ray mirror system [42,43]. We used a 10-μm-thick nanocrystal Si film (grain size of 500 nm, U.S. Research Nanomaterials) as the target. The Si film attached to a polyimide film was set to a helium closed-cycle cryostat with a cylindrical x-ray window made of carbon fiber reinforced plastics (CFRP). The sample was placed at the focus and continuously translated spatially so that each double pulse irradiated the undamaged surface. The diffraction peaks from the sample (111, 220, and 311 reflections) in the horizontal plane were measured by using a multiport charge-coupled device (MPCCD) detector [44] that covered the scattering angle (2θ) range of 20°–55°. The top half of the detector was covered by a 40-μm-thick copper foil such that the diffraction signals from the probe pulses selectively impinged on the detector, while a 600-μm-thick aluminum foil covered the bottom half of the detector to measure the diffraction signals from the pump pulses. The shot-by-shot pulse energy at the sample was characterized by using an inline spectrometer [45] located upstream of the focusing mirror system and taking into account the reflectivity of the mirrors and the transmittance of the CFPR window. The diffraction data at initial sample temperature $T = 10$, 100, and 300 K were collected by changing the delay time from 0.5 to 100 fs.

We extracted the detector data for double pulses with specific pulse energies of the pump (100 ± 20 μJ) and probe pulses (30 ± 20 μJ) and calculated the averaged diffraction profile for each temperature and delay time. The absorbed dose for the selected pump pulses was ∼10 eV/atom, which was much higher than the predicted damage threshold of Si (∼1 eV/atom) [30]. Figure 1(b) shows the probe diffraction profiles in the vicinity of each reflection peak for the experiment at $T = 300$ K. It is clearly seen that the diffraction intensity decreased with the delay time for each reflection index. We can consider two possible reasons for the ultrafast decay of the diffraction intensity: the change of atomic scattering factors and the progressing atomic disorder. The change of atomic scattering factors is caused by the photoionization and secondary ionizations [46–50]. Although the atomic scattering factors of the ionized atoms are mostly determined by the number of occupied core levels [51], the number of core holes per atom is here too small ($\sim 10^{-2}$ for the x-ray dose in the current experiment [27]) to explain the experimental observations. The only possible origin for the diffraction intensity decay is the progressing atomic disorder.

Since the Bragg diffraction angle for the probe pulses did not change for all delay times, it is natural to consider that the lattice constants did not change on the femtosecond timescale. In this case, the diffraction intensity may be proportional to $\exp(-q^2\langle u_{hkl}^2\rangle)$ with the mean square of the atomic displacement perpendicular to the (hkl) plane $\langle u_{hkl}^2\rangle$ and the scattering vector $q = 4\pi \sin\theta/\lambda$ with the wavelength λ, as an analogy to the Debye-Waller factor in crystallography.

We evaluated the atomic disorder from the measured diffraction profiles of the pump and probe pulses as follows. First, the background of the diffraction profiles of the probe pulses was estimated by fitting the profiles in the vicinity of diffraction peaks with polynomial functions [black dotted curves in Fig. 1(b)]. After subtracting the estimated background, each diffraction peak was fitted by a Gaussian function and the integrated diffraction intensity ($I_{111}^{\text{probe}}, I_{220}^{\text{probe}}, I_{311}^{\text{probe}}$) was determined. For comparing the probe diffraction intensity between different delay times, we compensated the inhomogeneity of the sample thickness and the differences in the probe pulse energy by calculating the diffraction efficiency of the probe pulses given by $I_{hkl} = \frac{I_{hkl}^{\text{probe}}/E^{\text{probe}}}{I_{220}^{\text{pump}}/E^{\text{pump}}}$, where hkl represents the reflection index, $E_{\text{pump(probe)}}$ is the average pulse energy of the pump (probe) pulses on the sample, and I_{220}^{pump} is the pump diffraction intensity of the 220 reflection evaluated by the same procedures for the pump diffraction intensity. Here, we used I_{220}^{pump}, rather than the pump diffraction intensity of other reflections, because the uncertainty of I_{220}^{pump} was smaller than those for other reflections. Figure 2 shows the probe diffraction efficiency as a function of delay time. Here, the diffraction efficiency for each initial sample temperature and for each reflection is normalized such that the averaged value for the short delay times (0.5–15 fs) equals the Debye-Waller factor $\exp(-q^2\langle u_0^2\rangle)$ for the undamaged Si calculated with $\langle u_0^2\rangle = 2.4 \times 10^{-3}$ Å^2 (10 K) [52], 3.2×10^{-3} Å^2 (100 K) [53], and 5.6×10^{-3} Å^2 (300 K) [53]. The vertical error bars represent the standard deviation of the diffraction efficiency calculated for five independent subensembles from the whole extracted pulses. The diffraction efficiency for all temperatures was almost the same at each delay time, indicating that thermal atomic motion in the equilibrium state is not related to the speed of the atomic disordering. A negligible contribution of the initial thermal atomic motion to the ultrafast melting can be also confirmed by comparing the experimental results and the diffraction efficiency predicted by the inertial model [28] given by

$$I_{hkl} = \begin{cases} \exp\left(-q^2\langle u_0^2\rangle\right) & \text{if } t \leqslant t_0, \\ \exp\left(-q^2\left(\langle u_0^2\rangle + v^2(t-t_0)^2\right)\right) & \text{otherwise,} \end{cases} \quad (1)$$

where t_0 is the onset time of the atomic displacement and $v = \sqrt{k_B T/m} = 5.4 \times 10^{-4}$ (10 K), 1.7×10^{-3} (100 K), and 3.0×10^{-3} Å/fs (300 K). Even if we select the onset to be $t_0 = 0$ fs, the diffraction efficiency predicted by the inertial model is higher than that observed in the experiment (Fig. 2).

Next, we discuss the thermal and nonthermal effects in the ultrafast melting by comparing the experimental results and theoretical simulations performed by using XTANT (x-ray-induced thermal and nonthermal transitions) code [54,55].

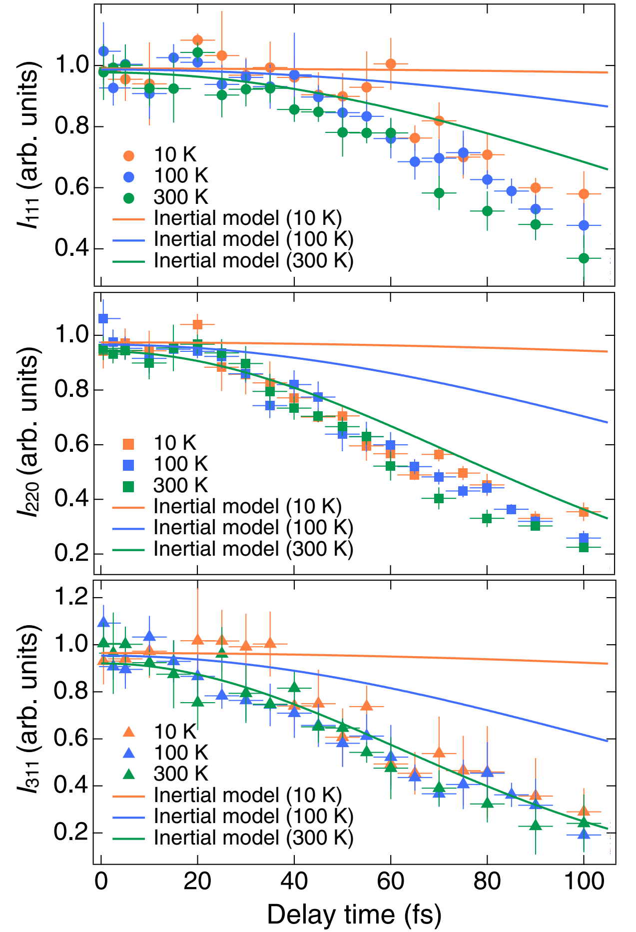

FIG. 2. Probe diffraction efficiency as a function of delay time for different sample temperatures (orange markers: 10 K; blue markers: 100 K; and green markers: 300 K). The solid curves represent the diffraction efficiency predicted by the inertial model.

First, we simulated the electron and ion temperatures of the x-ray-excited Si within and without the Born-Oppenheimer approximation (BO and non-BO simulations). In BO simulations, we simulate atomic movement solely under the modified interatomic potential, neglecting the phonon-mediated energy exchange between electrons and lattice. This simulation accounts only for nonthermal processes when following atomic movement. In contrast, non-BO simulations predict atomic movements under the modified interatomic potential while also accounting for the energy transfer from electrons to atoms (thermal process), which additionally heats up atoms. The calculation was performed for a 216-atom-large supercell at 300 K irradiated with a spatially uniform x-ray pulse of 2.5 fs duration (rms) and fluence corresponding to the average fluence in the experiment (pulse energy divided by the product of horizontal and vertical FWHM beam sizes). For both simulations, the ion temperature changes insignificantly during the first 10 fs after irradiation with the pump pulse. Then, the ion temperature quickly increases well above the original sample temperature [Fig. 3(a)], which is consistent with our experimental observation that the equilibrium atomic motion did not significantly contribute to the speed of atomic disordering. One major difference in the results for the two

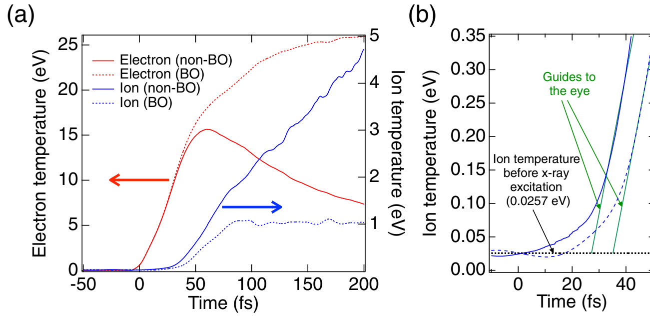

FIG. 3. (a) Simulated ion and electron temperatures in x-ray-excited silicon of initial temperature of 300 K. Time zero in the horizontal axis corresponds to the intensity maximum of the pump pulse. (b) Enlarged plot of the ion temperatures around time zero.

simulations is the onset time of the increase in ion temperature [Fig. 3(b)]; the ion temperature starts to rapidly increase at 25 fs after the x-ray exposure in the non-BO simulation, while the onset time of such a temperature increase is 35 fs in the BO simulation. These results suggest that both the thermal effect as well as the nonthermal effect may contribute to the progressing atomic disordering, i.e., the interplay between the thermal and nonthermal effects may be present in the x-ray-induced ultrafast melting.

The interplay of thermal and nonthermal effects to ultrafast melting can be investigated by comparing the simulated and experimentally measured onset times of atomic disordering. Figures 4(a)–4(c) show the rms atomic displacements perpendicular to the (hkl) plane $(hkl = 111, 220, 311)$ in the BO and the non-BO simulations of Si at 300 K performed with fluences of 100% [Fig. 4(a)], 48% [Fig. 4(b)], and 16% [Fig. 4(c)] of the average fluence in the experiment. For all fluence conditions and reflection indices, the onset time of

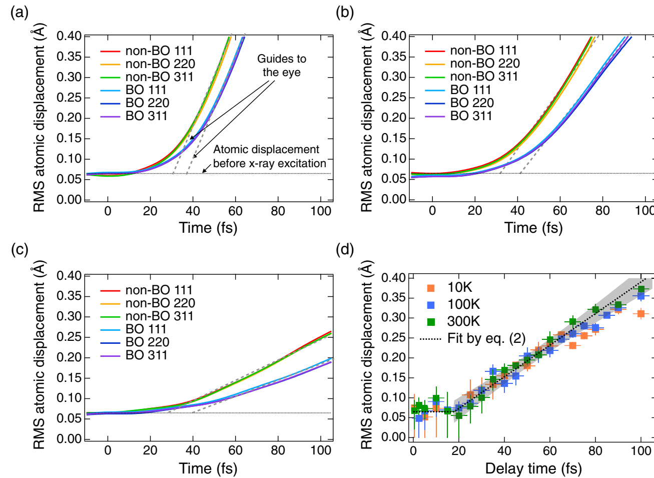

FIG. 4. (a)–(c) Root-mean-square atomic displacements perpendicular to the (111), (220), and (311) planes of silicon at 300 K predicted by non-BO and BO simulations with fluences of (a) 100%, (b) 48%, and (c) 16% of the average fluence in the experiment. (d) Experimentally observed root-mean-square atomic displacement perpendicular to the (220) plane of x-ray-excited silicon. The black dotted line is the fitting result by Eq. (2) and the gray shadow represents a 3-σ uncertainty band.

atomic disordering predicted by the non-BO simulation is 20–30 fs, which is approximately 10 fs faster than the predicted value in the BO simulation. Since the difference in the onset time is larger than the time resolution in the present experiment, our experimental data can be readily used to check the existence of thermal effects in ultrafast melting.

Figure 4(d) shows the experimentally observed rms atomic displacement perpendicular to the (220) plane ($\sqrt{\langle u_{220}^2\rangle}$) evaluated through the relationship $I_{220} = \exp(-q^2\langle u_{220}^2\rangle)$. The atomic displacement remains at its original value for the first few tens of femtoseconds after irradiation with the pump pulse and then increases with time. The time dependence of $\sqrt{\langle u_{220}^2\rangle}$ can be well described by

$$\sqrt{\langle u_{220}^2\rangle} = \begin{cases} \sqrt{\langle u_0^2\rangle} & \text{if } t \leqslant t_0, \\ \sqrt{\langle u_0^2\rangle} + v_{220}(t - t_0) & \text{otherwise,} \end{cases} \tag{2}$$

where v_{220} is the slope and t_0 is the onset time of atomic displacement. The green dotted line in Fig. 4(a) represents the fitting results of $\sqrt{\langle u_{220}^2\rangle}$ at 300 K by Eq. (2). t_0 was estimated to 18 ± 6 fs, which is consistent with the results of the non-BO simulation and not with those of the BO simulation. The consistency between the experiment and the non-BO simulation supports our claim that both thermal and nonthermal effects contribute to the x-ray-induced ultrafast melting. The atomic displacements perpendicular to the (111) and (311) planes, determined using the same procedure, are presented in the Supplemental Material [56]. However, the lower accuracy of diffraction efficiencies for the 111 and 311 reflections (as shown in Fig. 2) hinders the precise determination of the onset time of atomic displacements.

Although the non-BO simulation reproduces the onset time of atomic disordering as evaluated by the experiment, the predicted degree of atomic disorder for the average fluence [Fig. 4(a)] is higher than the experimentally measured values [Fig. 4(d)]. This discrepancy may be explained by the nonuniformity of the pump fluence. Since the focal spots of the pump and probe pulses had Gaussian shapes in the present experiment [42], the probe diffraction signals originated from various sample regions irradiated with different pump fluence. The simulation results shown in Figs. 4(a)–4(c) predict that the atomic disordering of crystals experiencing a higher pump fluence increases faster, implying that their contribution to the probe diffraction intensity decreases with time. Consequently, the "effective" pump fluence might be reduced with the increasing delay time in the present experiment. Summing up the scattering amplitude over the entire sample volume irradiated with the probe pulse, as done in our previous study [27], would require an extensive and long-taking computational effort, not bringing new aspects for the data understanding. We therefore leave it out of the present Letter.

In summary, we conducted an x-ray pump-x-ray probe experiment on Si and observed femtosecond structural changes under strong excitation conditions at various initial sample temperatures. The results of the experiment revealed that the onset time and rate of atomic disordering were not affected by the initial sample temperature, similarly as during the optically induced ultrafast melting of semiconductors under strong excitation [8]. The comparison of the onset time of

atomic displacement between experiment and simulation indicates an interplay of nonthermal and thermal effects in x-ray-induced ultrafast melting. Accurate modeling of the x-ray-matter interaction including the nonthermal and thermal effects will be helpful for the planning and proper interpretation of various experiments utilizing focused XFEL pulses, such as molecular imaging [57], protein nanocrystallography [18], generation of warm-dense matter and plasma in the high-energy-density regime [58], and the investigation and applications of nonlinear x-ray-matter interaction processes [59–62].

The work was supported by the Japan Society for the Promotion of Science (JSPS) KAKENHI Grants (No. 19K20604, No. 19KK0132, No. 20H04656, No. 21H05235, No. 22H03877, and No. 22KK0233). K.J.K. thanks the Polish National Agency for Academic Exchange for funding in the frame of the Bekker programme (PPN/BEK/2020/1/00184) and of its National Component (BPN/BKK/2022/1/00011). H.J.L. and P.H. acknowledge funding from the U.S. Department of Energy Office of Science, Fusion Energy Science under Contract No. DE-AC02-76SF00515, FWP 100106.

[1] C. V. Shank, R. Yen, and C. Hirlimann, Time-resolved reflectivity measurements of femtosecond-optical-pulse-induced phase transitions in silicon, Phys. Rev. Lett. **50**, 454 (1983).

[2] C. V. Shank, R. Yen, and C. Hirlimann, Femtosecond-time-resolved surface structural dynamics of optically excited silicon, Phys. Rev. Lett. **51**, 900 (1983).

[3] E. N. Glezer, Y. Siegal, L. Huang, and E. Mazur, Behavior of $\chi^{(2)}$ during a laser-induced phase transition in GaAs, Phys. Rev. B **51**, 9589 (1995).

[4] C. W. Siders, A. Cavalleri, K. Sokolowski-Tinten, C. Tóth, T. Guo, M. Kammler, M. H. von Hoegen, K. R. Wilson, D. von der Linde, and C. P. J. Barty, Detection of nonthermal melting by ultrafast x-ray diffraction, Science **286**, 1340 (1999).

[5] A. Rousse, C. Rischel, S. Fourmaux, I. Uschmann, S. Sebban, G. Grillon, P. Balcou, E. Förster, J. P. Geindre, P. Audebert, J. C. Gauthier, and D. Hulin, Non-thermal melting in semiconductors measured at femtosecond resolution, Nature (London) **410**, 65 (2001).

[6] K. Sokolowski-Tinten, C. Blome, C. Dietrich, A. Tarasevitch, M. Horn von Hoegen, D. von der Linde, A. Cavalleri, J. Squier, and M. Kammler, Femtosecond x-ray measurement of ultrafast melting and large acoustic transients, Phys. Rev. Lett. **87**, 225701 (2001).

[7] A. M. Lindenberg, J. Larsson, K. Sokolowski-Tinten, K. J. Gaffney, C. Blome, O. Synnergren, J. Sheppard, C. Caleman, A. G. MacPhee, D. Weinstein, D. P. Lowney, T. K. Allison, T. Matthews, R. W. Falcone, A. L. Cavalieri, D. M. Fritz, S. H. Lee, P. H. Bucksbaum, D. A. Reis, J. Rudati *et al.*, Atomic-scale visualization of inertial dynamics, Science **308**, 392 (2005).

[8] K. J. Gaffney, A. M. Lindenberg, J. Larsson, K. Sokolowski-Tinten, C. Blome, O. Synnergren, J. Sheppard, C. Caleman, A. G. MacPhee, D. Weinstein, D. P. Lowney, T. Allison, T. Matthews, R. W. Falcone, A. L. Cavalieri, D. M. Fritz, S. H. Lee, P. H. Bucksbaum, D. A. Reis, J. Rudati *et al.*, Observation of structural anisotropy and the onset of liquidlike motion during the nonthermal melting of InSb, Phys. Rev. Lett. **95**, 125701 (2005).

[9] P. B. Hillyard, K. J. Gaffney, A. M. Lindenberg, S. Engemann, R. A. Akre, J. Arthur, C. Blome, P. H. Bucksbaum, A. L. Cavalieri, A. Deb, R. W. Falcone, D. M. Fritz, P. H. Fuoss, J. Hajdu, P. Krejcik, J. Larsson, S. H. Lee, D. A. Meyer, A. J. Nelson, R. Pahl *et al.*, Carrier-density-dependent lattice stability in InSb, Phys. Rev. Lett. **98**, 125501 (2007).

[10] M. Harb, R. Ernstorfer, C. T. Hebeisen, G. Sciaini, W. Peng, T. Dartigalongue, M. A. Eriksson, M. G. Lagally, S. G. Kruglik, and R. J. D. Miller, Electronically driven structure changes of Si captured by femtosecond electron diffraction, Phys. Rev. Lett. **100**, 155504 (2008).

[11] X. Wang, J. C. Ekström, A. U. J. Bengtsson, A. Jarnac, A. Jurgilaitis, V.-T. Pham, D. Kroon, H. Enquist, and J. Larsson, Role of thermal equilibrium dynamics in atomic motion during nonthermal laser-induced melting, Phys. Rev. Lett. **124**, 105701 (2020).

[12] Å. U. J. Bengtsson, J. C. Ekström, X. Wang, A. Jurgilaitis, V.-T. Pham, D. Kroon, and J. Larsson, Repetitive non-thermal melting as a timing monitor for femtosecond pump/probe x-ray experiments, Struct. Dyn. **7**, 054303 (2020).

[13] E. Möhr-Vorobeva, S. L. Johnson, P. Beaud, U. Staub, R. De Souza, C. Milne, G. Ingold, J. Demsar, H. Schaefer, and A. Titov, Nonthermal melting of a charge density wave in $TiSe_2$, Phys. Rev. Lett. **107**, 036403 (2011).

[14] M. Porer, U. Leierseder, J. M. Ménard, H. Dachraoui, L. Mouchliadis, I. E. Perakis, U. Heinzmann, J. Demsar, K. Rossnagel, and R. Huber, Non-thermal separation of electronic and structural orders in a persisting charge density wave, Nat. Mater. **13**, 857 (2014).

[15] S. K. Sundaram and E. Mazur, Inducing and probing non-thermal transitions in semiconductors using femtosecond laser pulses, Nat. Mater. **1**, 217 (2002).

[16] B. W. J. McNeil and N. R. Thompson, X-ray free-electron lasers, Nat. Photon. **4**, 814 (2010).

[17] C. Pellegrini, A. Marinelli, and S. Reiche, The physics of x-ray free-electron lasers, Rev. Mod. Phys. **88**, 015006 (2016).

[18] H. N. Chapman, P. Fromme, A. Barty, T. A. White, R. A. Kirian, A. Aquila, M. S. Hunter, J. Schulz, D. P. DePonte, U. Weierstall, R. B. Doak, F. R. N. C. Maia, A. V. Martin, I. Schlichting, L. Lomb, N. Coppola, R. L. Shoeman, S. W. Epp, R. Hartmann, D. Rolles *et al.*, Femtosecond x-ray protein nanocrystallography, Nature (London) **470**, 73 (2011).

[19] I. Schlichting, Serial femtosecond crystallography: The first five years, IUCrJ **2**, 246 (2015).

[20] R. L. Owen, E. Rudiño-Piñera, and E. F. Garman, Experimental determination of the radiation dose limit for cryocooled protein crystals, Proc. Natl. Acad. Sci. USA **103**, 4912 (2006).

[21] M. R. Howells, T. Beetz, H. N. Chapman, C. Cui, J. M. Holton, C. J. Jacobsen, J. Kirz, E. Lima, S. Marchesini, H. Miao, D. Sayre, D. A. Shapiro, J. C. H. Spence, and D. Starodub, An assessment of the resolution limitation due to radiation-damage in x-ray diffraction microscopy, J. Electron Spectrosc. Relat. Phenom. **170**, 4 (2009).

[22] E. F. Garman, Radiation damage in macromolecular crystallography: What is it and why should we care? Acta Crystallogr. Sect. D **66**, 339 (2010).

[23] J. M. Holton and K. A. Frankel, The minimum crystal size needed for a complete diffraction data set, Acta Crystallogr. Sect. D **66**, 393 (2010).

[24] H. N. Chapman, C. Caleman, and N. Timneanu, Diffraction before destruction, Philos. Trans. R. Soc. B **369**, 20130313 (2014).

[25] N. Medvedev and B. Ziaja, Multistep transition of diamond to warm dense matter state revealed by femtosecond x-ray diffraction, Sci. Rep. **8**, 5284 (2018).

[26] I. Inoue, Y. Deguchi, B. Ziaja, T. Osaka, M. M. Abdullah, Z. Jurek, N. Medvedev, V. Tkachenko, Y. Inubushi, H. Kasai, K. Tamasaku, T. Hara, E. Nishibori, and M. Yabashi, Atomic-scale visualization of ultrafast bond breaking in x-ray-excited diamond, Phys. Rev. Lett. **126**, 117403 (2021).

[27] V. Tkachenko, M. M. Abdullah, Z. Jurek, N. Medvedev, V. Lipp, M. Makita, and B. Ziaja, Limitations of structural insight into ultrafast melting of solid materials with x-ray diffraction imaging, Appl. Sci. **11**, 5157 (2021).

[28] T. Pardini, J. Alameda, A. Aquila, S. Boutet, T. Decker, A. E. Gleason, S. Guillet, P. Hamilton, M. Hayes, R. Hill, J. Koglin, B. Kozioziemski, J. Robinson, K. Sokolowski-Tinten, R. Soufli, and S. P. Hau-Riege, Delayed onset of nonthermal melting in single-crystal silicon pumped with hard x rays, Phys. Rev. Lett. **120**, 265701 (2018).

[29] N. J. Hartley, J. Grenzer, L. Huang, Y. Inubushi, N. Kamimura, K. Katagiri, R. Kodama, A. Kon, W. Lu, M. Makita, T. Matsuoka, S. Nakajima, N. Ozaki, T. Pikuz, A. V. Rode, D. Sagae, A. K. Schuster, K. Tono, K. Voigt, J. Vorberger *et al.*, Using diffuse scattering to observe x-ray-driven nonthermal melting, Phys. Rev. Lett. **126**, 015703 (2021).

[30] N. Medvedev, Z. Li, and B. Ziaja, Thermal and nonthermal melting of silicon under femtosecond x-ray irradiation, Phys. Rev. B **91**, 054113 (2015).

[31] N. Medvedev, Z. Fang, C. Xia, and Z. Li, Thermal and nonthermal melting of III-V compound semiconductors, Phys. Rev. B **99**, 144101 (2019).

[32] N. Medvedev, Nonthermal phase transitions in irradiated oxides, J. Phys.: Condens. Matter **32**, 435401 (2020).

[33] I. Inoue, Y. Inubushi, T. Sato, K. Tono, T. Katayama, T. Kameshima, K. Ogawa, T. Togashi, S. Owada, Y. Amemiya, T. Tanaka, T. Hara, and M. Yabashi, Observation of femtosecond X-ray interactions with matter using an X-ray–X-ray pump–probe scheme, Proc. Natl. Acad. Sci. USA **113**, 1492 (2016).

[34] I. Inoue, V. Tkachenko, K. J. Kapcia, V. Lipp, B. Ziaja, Y. Inubushi, T. Hara, M. Yabashi, and E. Nishibori, Delayed onset and directionality of x-ray-induced atomic displacements observed on subatomic length scales, Phys. Rev. Lett. **128**, 223203 (2022).

[35] T. Ishikawa, H. Aoyagi, T. Asaka, Y. Asano, N. Azumi, T. Bizen, H. Ego, K. Fukami, T. Fukui, Y. Furukawa, S. Goto, H. Hanaki, T. Hara, T. Hasegawa, T. Hatsui, A. Higashiya, T. Hirono, N. Hosoda, M. Ishii, T. Inagaki *et al.*, A compact x-ray free-electron laser emitting in the sub-ångström region, Nat. Photon. **6**, 540 (2012).

[36] Y. Inubushi, I. Inoue, J. Kim, A. Nishihara, S. Matsuyama, H. Yumoto, T. Koyama, K. Tono, H. Ohashi, K. Yamauchi, and M. Yabashi, Measurement of the x-ray spectrum of a free electron laser with a wide-range high-resolution single-shot spectrometer, Appl. Sci. **7**, 584 (2017).

[37] I. Inoue, T. Hara, Y. Inubushi, K. Tono, T. Inagaki, T. Katayama, Y. Amemiya, H. Tanaka, and M. Yabashi, X-ray Hanbury Brown–Twiss interferometry for determination of ultrashort electron-bunch duration, Phys. Rev. Accel. Beams **21**, 080704 (2018).

[38] I. Inoue, K. Tamasaku, T. Osaka, Y. Inubushi, and M. Yabashi, Determination of x-ray pulse duration via intensity correlation measurements of x-ray fluorescence, J. Synchrotron Radiat. **26**, 2050 (2019).

[39] T. Osaka, I. Inoue, J. Yamada, Y. Inubushi, S. Matsumura, Y. Sano, K. Tono, K. Yamauchi, K. Tamasaku, and M. Yabashi, Hard x-ray intensity autocorrelation using direct two-photon absorption, Phys. Rev. Res. **4**, L012035 (2022).

[40] M. Yabashi, H. Tanaka, and T. Ishikawa, Overview of the SACLA facility, J. Synchrotron Radiat. **22**, 477 (2015).

[41] T. Hara, Y. Inubushi, T. Katayama, T. Sato, H. Tanaka, T. Tanaka, T. Togashi, K. Togawa, K. Tono, M. Yabashi, and T. Ishikawa, Two-colour hard x-ray free-electron laser with wide tunability, Nat. Commun. **4**, 2919 (2013).

[42] H. Yumoto, H. Mimura, T. Koyama, S. Matsuyama, K. Tono, T. Togashi, Y. Inubushi, T. Sato, T. Tanaka, T. Kimura, H. Yokoyama, J. Kim, Y. Sano, Y. Hachisu, M. Yabashi, H. Ohashi, H. Ohmori, T. Ishikawa, and K. Yamauchi, Focusing of x-ray free-electron laser pulses with reflective optics, Nat. Photon. **7**, 43 (2013).

[43] K. Tono, T. Togashi, Y. Inubushi, T. Katayama, S. Owada, T. Yabuuchi, A. Kon, I. Inoue, T. Osaka, H. Yumoto, T. Koyama, H. Ohashi, and M. Yabashi, Overview of optics, photon diagnostics and experimental instruments at SACLA: Development, operation and scientific applications, Proc. SPIE **10237**, 1023706 (2017).

[44] T. Kameshima, S. Ono, T. Kudo, K. Ozaki, Y. Kirihara, K. Kobayashi, Y. Inubushi, M. Yabashi, T. Horigome, A. Holland, K. Holland, D. Burt, H. Murao, and T. Hatsui, Development of an x-ray pixel detector with multi-port charge-coupled device for x-ray free-electron laser experiments, Rev. Sci. Instrum. **85**, 033110 (2014).

[45] K. Tamasaku, Y. Inubushi, I. Inoue, K. Tono, M. Yabashi, and T. Ishikawa, Inline spectrometer for shot-by-shot determination of pulse energies of a two-color x-ray free-electron laser, J. Synchrotron Radiat. **23**, 331 (2016).

[46] B. Ziaja, D. van der Spoel, A. Szöke, and J. Hajdu, Auger-electron cascades in diamond and amorphous carbon, Phys. Rev. B **64**, 214104 (2001).

[47] B. Ziaja, R. A. London, and J. Hajdu, Unified model of secondary electron cascades in diamond, J. Appl. Phys. **97**, 064905 (2005).

[48] S.-K. Son, L. Young, and R. Santra, Impact of hollow-atom formation on coherent x-ray scattering at high intensity, Phys. Rev. A **83**, 033402 (2011).

[49] B. Ziaja, Z. Jurek, N. Medvedev, V. Saxena, S.-K. Son, and R. Santra, Towards realistic simulations of macromolecules irradiated under the conditions of coherent diffraction imaging with an x-ray free-electron laser, Photonics **2**, 256 (2015).

[50] I. Inoue, J. Yamada, K. J. Kapcia, M. Stransky, V. Tkachenko, Z. Jurek, T. Inoue, T. Osaka, Y. Inubushi, A. Ito, Y. Tanaka, S. Matsuyama, K. Yamauchi, M. Yabashi, and B. Ziaja, Femtosecond reduction of atomic scattering factors triggered by intense x-ray pulse, Phys. Rev. Lett. **131**, 163201 (2023).

[51] S. P. Hau-Riege, X-ray atomic scattering factors of low-*Z* ions with a core hole, Phys. Rev. A **76**, 042511 (2007).

[52] J. S. Reid and J. D. Pirie, Dynamic deformation and the Debye–Waller factors for silicon-like crystals, Acta Crystallogr. Sect. A **36**, 957 (1980).

[53] N. Wahlberg, N. Bindzus, L. Bjerg, J. Becker, A.-C. Dippel, and B. B. Iversen, Synchrotron powder diffraction of silicon: High-quality structure factors and electron density, Acta Crystallogr. Sect. A **72**, 28 (2016).

[54] N. Medvedev, H. O. Jeschke, and B. Ziaja, Nonthermal phase transitions in semiconductors induced by a femtosecond extreme ultraviolet laser pulse, New J. Phys. **15**, 015016 (2013).

[55] N. Medvedev, V. Tkachenko, V. Lipp, Z. Li, and B. Ziaja, Various damage mechanisms in carbon and silicon materials under femtosecond x-ray irradiation, 4Open **1**, 3 (2018).

[56] See Supplemental Material at http://link.aps.org/supplemental/10.1103/PhysRevB.110.L100102 for atomic displacements in x-ray-excited silicon.

[57] R. Neutze, R. Wouts, D. van der Spoel, E. Weckert, and J. Hajdu, Potential for biomolecular imaging with femtosecond x-ray pulses, Nature (London) **406**, 752 (2000).

[58] S. M. Vinko, O. Ciricosta, B. I. Cho, K. Engelhorn, H. K. Chung, C. R. D. Brown, T. Burian, J. Chalupský, R. W. Falcone, C. Graves, V. Hájková, A. Higginbotham, L. Juha, J. Krzywinski, H. J. Lee, M. Messerschmidt, C. D. Murphy, Y. Ping, A. Scherz, W. Schlotter *et al.*, Creation and diagnosis of a solid-density plasma with an x-ray free-electron laser, Nature (London) **482**, 59 (2012).

[59] H. Yoneda, Y. Inubushi, K. Nagamine, Y. Michine, H. Ohashi, H. Yumoto, K. Yamauchi, H. Mimura, H. Kitamura, T. Katayama, T. Ishikawa, and M. Yabashi, Atomic inner-shell laser at 1.5-ångström wavelength pumped by an x-ray free-electron laser, Nature (London) **524**, 446 (2015).

[60] K. Tamasaku, E. Shigemasa, Y. Inubushi, T. Katayama, K. Sawada, H. Yumoto, H. Ohashi, H. Mimura, M. Yabashi, K. Yamauchi, and T. Ishikawa, X-ray two-photon absorption competing against single and sequential multiphoton processes, Nat. Photon. **8**, 313 (2014).

[61] K. Tamasaku, E. Shigemasa, Y. Inubushi, I. Inoue, T. Osaka, T. Katayama, M. Yabashi, A. Koide, T. Yokoyama, and T. Ishikawa, Nonlinear spectroscopy with x-ray two-photon absorption in metallic copper, Phys. Rev. Lett. **121**, 083901 (2018).

[62] I. Inoue, Y. Inubushi, T. Osaka, J. Yamada, K. Tamasaku, H. Yoneda, and M. Yabashi, Shortening x-ray pulse duration via saturable absorption, Phys. Rev. Lett. **127**, 163903 (2021).